Upconversion Luminescence-Activated DNA Nanodevice for ATP Sensing in Living Cells

Jian Zhao,[†,#] Jinhong Gao,[†,#] Wenting Xue,[†] Zhenghan Di,[†] Hang Xing,[‡] Yi Lu,[§] and Lele Li,[*,†]

[†]CAS Key Laboratory for Biomedical Effects of Nanomaterials and Nanosafety and CAS Center for Excellence in Nanoscience, National Center for Nanoscience and Technology, Beijing 100190, China

[‡]Institute of Chemical Biology and Nanomedicine, College of Chemistry and Chemical Engineering, Hunan University, Changsha, Hunan 410082, China

[§]Department of Chemistry, University of Illinois at Urbana-Champaign, Urbana, Illinois 61801, United States

MATERIALS AND METHODS

Materials: All of the chemicals were used as received without further purification. Rare Earth Oxides, oleylamine (OM, 90%), and 1-octadecene (ODE, 95%) were purchased from Acros. Oleic acid (OA, 90%) and trifluoroacetic acid (99%) were bought from Sigma-Aldrich. The labeled DNA (see Table S1) were synthesized and purified by Sangon Biotech Co. (Shanghai, China). The water used throughout the experiments was Millipore water (18.2 MΩ). All the experiments were conducted in room temperature unless mentioned otherwise.

Instrumentations: The UV-vis spectra were obtained from a Hitachi 5300 spectrophotometer (Hitachi Co. Ltd., Japan). Fluorescence spectra were collected using a Hitachi F-4600 fluorimeter (Hitachi Co. Ltd., Japan). The transmission electron microscopic (TEM) and high-resolution transmission microscopic (HR-TEM) images were obtained using a Hitachi HT-7700 (Hitachi Co. Ltd., Japan) and Tecnai F20 transmission electron microscope, respectively. The hydrodynamic diameter and ζ-potentials of nanoparticles were obtained using Malvern nano ZS90. Confocal microscopic images were obtained using a Zeiss LSM 710 confocal microscope at 63× magnification. Cell viability data were obtained using a Biotech Epoch2 microreader. The nanoparticles of cellular uptake were obtained using a BD Accuri C6 Flow cytometry. The in vivo fluorescence images were obtained from a KODAK In-Vivo Imaging System FX Pro.

Synthesis of $NaGdF_4$:Yb/Tm: The upconversion nanoparticles (UCNPs) were synthesized according to a modified thermal decomposition method.[1,2] To a three-necked flask (100 mL) containing a mixture of oleic acid (OA), oleylamine (OM), 1-octadecene (ODE) (40 mmol, molar ratio: 1:1:2), a given amount of $Ln(CF_3COO)_3$ [1 mmol, 0.29 mmol $Gd(CF_3COO)_3$, 0.70 mmol $Yb(CF_3COO)_3$, and 0.01 mmol $Tm(CF_3COO)_3$], and CF_3COONa (1 mmol) were added at room temperature. The slurry was heated to 120 ˚C to remove low-boiling component and oxygen with vigorous stirring under vacuum. Then, the solution was heated to 320 ˚C and kept for 30 min under N_2 atmosphere. After cooling to room temperature, the products

were precipitated out by the addition of ethanol, collected by centrifugation, and re-dispersed in 10 mL of cyclohexane. Then, to a three-necked flask (100 mL) containing 5 mL as-prepared nanoparticles, a given amount of $Ln(CF_3COO)_3$ [0.5 mmol, 0.145 mmol $Gd(CF_3COO)_3$, 0.35 mmol $Yb(CF_3COO)_3$, and 0.005 mmol $Tm(CF_3COO)_3$], and CF_3COONa (0.5 mmol) were added at room temperature. The slurry was heated to 120 ˚C to remove low-boiling component and oxygen with vigorous stirring under vacuum. Then, the solution was heated to 320 ˚C and kept for 50 min under N_2 atmosphere. After cooling to room temperature, the $NaGdF_4$:Yb/Tm NPs were precipitated out by the addition of ethanol, collected by centrifugation, and re-dispersed in 10 mL of cyclohexane.

Synthesis of core-shell $NaGdF_4$:Yb/Tm@$NaGdF_4$: To a three-necked flask (100 mL) containing 10 mL as-prepared $NaGdF_4$:Yb/Tm, a given amount of $Ln(CF_3COO)_3$ [2 mmol $Gd(CF_3COO)_3$ and CF_3COONa (2 mmol) were added at room temperature. The slurry was heated to 120 ˚C to remove low-boiling component and oxygen with vigorous stirring under vacuum. Then, the solution was heated to 320 ˚C and kept for 50 min under N_2 atmosphere. After cooling to room temperature, the $NaGdF_4$:Yb/Tm@$NaGdF_4$ UCNPs were precipitated out by the addition of ethanol, collected by centrifugation, and re-dispersed in 10 mL of cyclohexane.

Calculation of molar concentration of UCNPs: The molecular concentration of the UCNPs was determined using two data: the mass of total UCNPs in solution (obtained from ICP-MS data of lanthanide element) and the mass of a single UCNP. The volume of a single UCNP was obtained with TEM characterization, and the mass of a single UCNP could be calculated by multiplying this volume with the density of $NaGdF_4$ (5.65 g/cm^3)[3].

Preparation of Apt-Act probes: Apt-Act probes were obtained by hybridization of aptamer strand with PC-inhibitor strand. Briefly, Apt-Act stock solution was prepared by adding quencher-modified PC-inhibitor

to a buffer solution (20 mM HEPES, 150 mM NaCl, 5 mM $MgCl_2$ pH 7.4) of Cy3-labeled aptamer strand with a final ratio of 1:1. The solution was annealed and stored at room temperature to allow full hybridization.

ATP sensing assay: The Apt-Act probes were diluted to 100 nM for ATP sensing assay. To the diluted probes (Apt-Act, Apt-on or Apt-non), different amounts of concentrated ATP solution was added. The mixtures were vortexed and incubated for 20 min. The fluorescence spectra were collected with excitation wavelength at 530 nm. For the UV-activated sensing assay, the Apt-Act or the control probes were irradiated with a UV lamp (5 mW/cm^2) followed by adding ATP and fluorescence spectra collection. In the case of selectivity assay, GTP, UTP, and CTP were used instead of ATP.

Preparation of Apt-Act/UCNPs: The as-prepared oleic-acid (OA) capped UCNPs (25mg) were dispersed in a mixture solution (water/ethanol = 1:1) containing HCl (0.05 M), and ultrasonicated for 10 min followed by stirring at room temperature for 2 h to remove the OA molecules on their surface. The OA-free UCNPs were collected by centrifugation, washed with acidic ethanol solution (pH <4) and deionized water several times, and re-dispersed in 1 mL deionized water. Then, 10 mg UCNPs were added to a water solution (500 μL) of PDL (20 mg), the resulting mixture was ultrasonicated for 10 min followed by stirring at room temperature for 24 h. Thereafter, the obtained UCNP-PDL was separated by centrifugation and washed several times with water. Finally, Apt-Act probes were incubated with UCNP-PDL with a molar ratio of 35:1 in a HEPES buffer (20 mM, 150 mM NaCl, 5 mM $MgCl_2$ pH 7.4), and the obtained Apt-Act/UCNPs was purified by centrifugation and washed several times with the HEPES buffer. The Apt-Act/UCNPs were dispersed in the HEPES buffer for further use.

Quantification of DNA surface density: The surface density of DNA probe on the nanodevices were determined by using Cy3-labeled Apt-Act (without labeling with quencher). After incubation of Cy3-labeled Apt-Act with UCNP-PDL in the HEPES buffer, the Apt-Act/UCNPs were then centrifuged and washed with

HEPES buffer. All the washing solutions were collected and the loading of Apt-Act was calculated from the difference of the Apt-Act concentration in the initial and collected solution by fluorescence measurement.

Cell culture: HeLa cells were used in all cell experiments. The cells were cultured in Dulbecoo's modification of Eagle's medium (DMEM) supplemented with 10% Fetal Bovine Serum (FBS), 100 U/mL penicillin, and 100 μg/mL streptomycin in a 5% CO_2, 37 °C incubator.

Cell viability test: HeLa cells were seeded in 96-well plate at a density of 2×10^4 cells/well. After 24 h incubation, cells were treated with Apt-Act/UCNPs (6.4 nM) for 2 h. After irradiation with 980 nm NIR laser for 20 min (1.2 W cm^{-2}, 5 min break after 1.5 min irradiation), cells were maintained for another 16 h. Finally, CCK-8 (Beyotime) assay was tested and absorbance at 450 nm was obtained with Epoch 2 microplate reader. Cells without any treatment were used as negative control.

Analysis of NIR-activated sensing in live cells by confocal microscopy: HeLa cells were seeded in 35 mm glass-bottom confocal dish (2×10^5 cells/well) and incubated for 24 h. DMEM medium was replaced with 500 μL Opti-MEM medium containing 6.4 nM Apt-Act/UCNPs or control nanoprobes. After 2 h incubation, the cells were washed thoroughly with PBS for 5 times, and 500 μL Opti-MEM medium was replenished. Then the cells were irradiated with 980 nm laser for 20 min (1.2 W cm^{-2}, 5 min break after 1.5 min irradiation). After another 1 h incubation, the post treatment cells were collected for fluorescence imaging. Lysotracker and Mitotracker were used to specifically stain the lysosomes and mitochondria of cells according to manufacturer protocol, respectively. The cells were incubated with 100 μM iodoacetic acid (IAA) at 37 °C for 4 h to decrease ATP generation by inhibiting glycolysis within cells,[4] then the cells were used for NIR-activated sensing and imaging. During the imaging process, the pinhole and gain setting were kept constant for all the samples.

Flow cytometry: HeLa cells were seeded in 6-well plates (2×10^5 cells/well) and incubated for another 20 h to

reach ~80% confluence. DMEM medium was replaced with 500 μL Opti-MEM medium containing 6.4 nM Apt-Act/UCNPs or Apt-non/UCNPs. After 2 h incubation, the cells were washed thoroughly with PBS for 5 times and fresh Opti-MEM medium was replenished. Then the cells were irradiated with 980 nm laser for 20 min (1.2 W cm^{-2}, 5 min break after 1.5 min irradiation). After another 1 h incubation, the post treatment cells were detached with 0.25 % (w/v) trypsin and washed twice with PBS before flow cytometry assay.

In vivo imaging: For in vivo imaging, aptamer strand bearing Cy5 fluorophore was used instead of Cy3-labeled one to afford Apt-Act and Apt-non. All animal experiments were performed under the Guide for Care and Use of Laboratory Animals and were approved by the Institutional Animal Care and Use Committee (IACUC) of National Center for Nanoscience and Technology (NCNST). The female BALB/c (nu/nu) nude mice (16-18 g) from Beijing Vital River Laboratory Animal Technology Co. Ltd were used to set up tumor xenograft model. HeLa cells (1×10^6 cells/100 μL in 1:1 (v/v) PBS and Matrigel) were injected subcutaneously into the back of the mouse. Tumor length and width were measured with calipers, and the tumor volume (V) was calculated using the following equation: V = length × width × width/2. When the tumors grew to 200-400 mm^3, the mice were randomly divided into four groups for the treatment with Apt-Act/UCNPs, Apt-non/UCNPs, Apt-Act/UCNPs + NIR, Apt-non/UCNPs + NIR. The mice were intratumoral injected with Apt-Act/UCNPs or Apt-non/UCNPs at an DNA probe dose of 25 nmol/kg. In light-activation experiments, NIR treatment was performed 30 min post-injection by irradiating the tumour regions with a 980-nm laser for 20 min (1.2 W cm^{-2}, 5 min break after 1.5 min irradiation). Mice were anesthetized with isoflurane and imaged at specified time intervals post-treatment. Whole-body fluorescence imaging was performed with a KODAK In-Vivo Imaging System with excitation and emission wavelengths of 630 and 680 nm, respectively.

Table S1. The sequence of oligonucleotides used in this study.

	Sequence of DNA (from left to right: 5' to 3')
Cy3-labeled aptamer strand	Cy3-CAGTCACCTGGGGGAGTATTGCGGAGGAAGGT
Quencher-labeled PC-inhibitor	GCAATACTCC***PC***CCCAGGTGACTG-BHQ2
Quencher-labeled control strand that does not contain PC groups spaced part	CCCAGGTGACTG-BHQ2
nonPC-inhibitor	GCAATACTCCCCCAGGTGACTG-BHQ2
Cy5-labeled mutated aptamer strand	Cy5-CAGTCACCTGGGGGAGTATTGCAAAAACAGGT

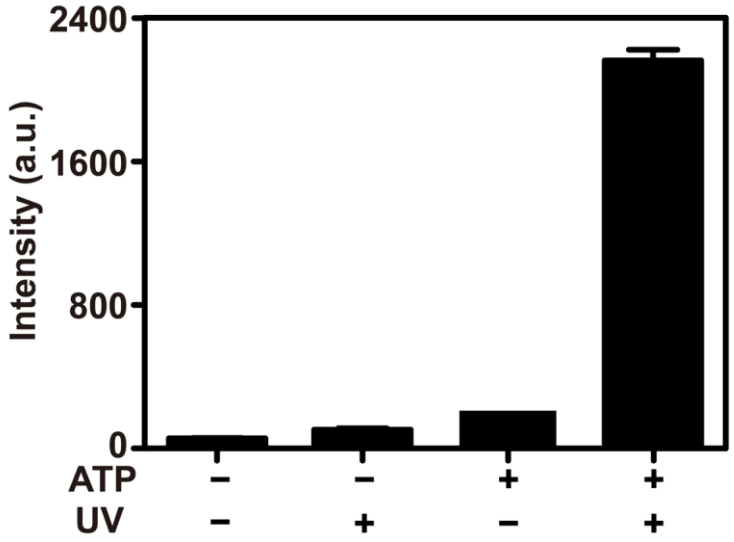

Figure S1. Response of the Apt-Act probe to ATP (5 mM) and UV light (365 nm).

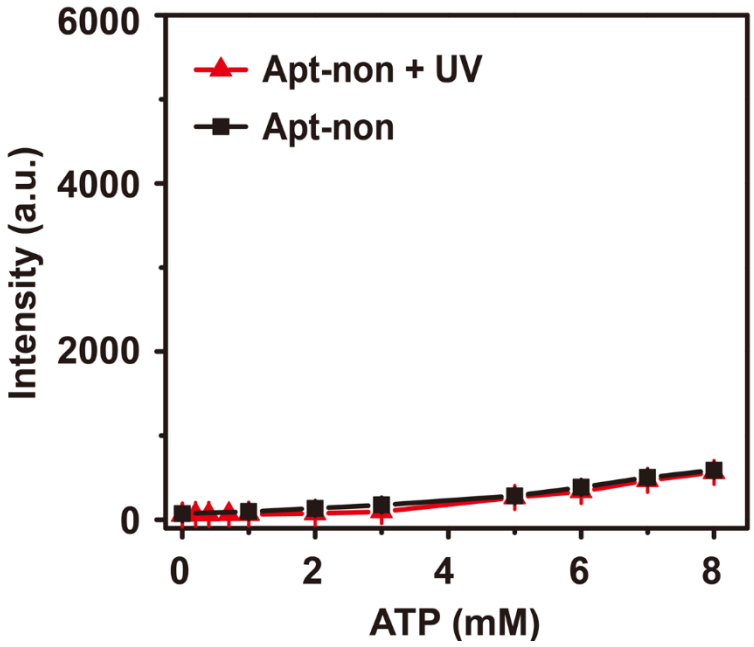

Figure S2. Fluorescence titration curve of the Apt-non probe for ATP with and without the 365 nm light irradiation.

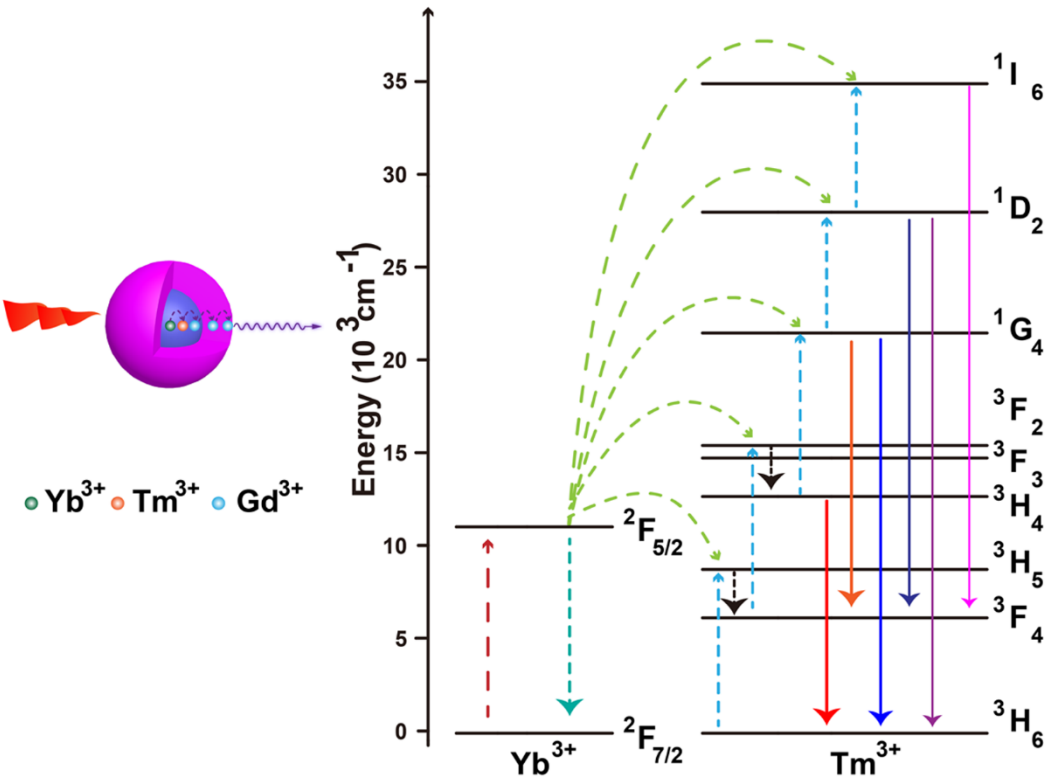

Figure S3. (left) Illustration of energy transfer mechanism of the core-shell $NaGdF_4$:Yb/Tm@$NaGdF_4$ UCNPs. Note that the core and shell regions are featured in different color, and the energy transfer occurs through the Yb→Tm→Gd pathway upon 980 nm excitation. (right) Energy level diagrams of the Yb^{3+}, Tm^{3+} ions and the energy transfer mechanism of $NaGdF_4$:Yb/Tm in the energy level. The core-shell design could also efficiently avoid surface quenching-induced energy loss of the active dopants (Yb/Tm) in the core and ensure high upconversion efficiency.[5]

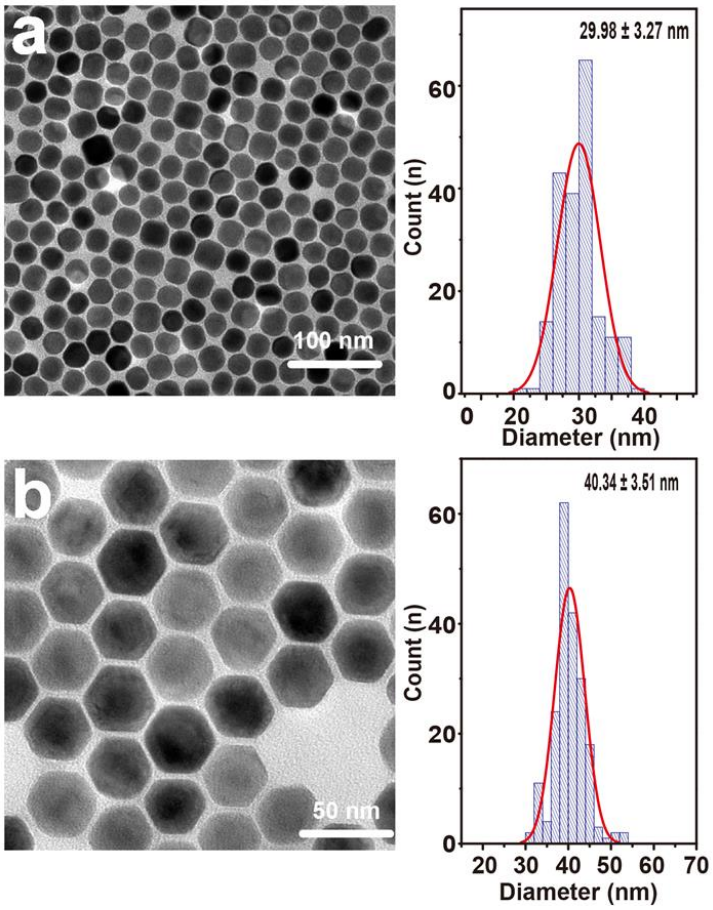

Figure S4. TEM image (left) and corresponding size distribution (right) of the (a) $NaGdF_4$:Yb/Tm core and (b) $NaGdF_4$:Yb/Tm@$NaGdF_4$ core-shell UCNPs.

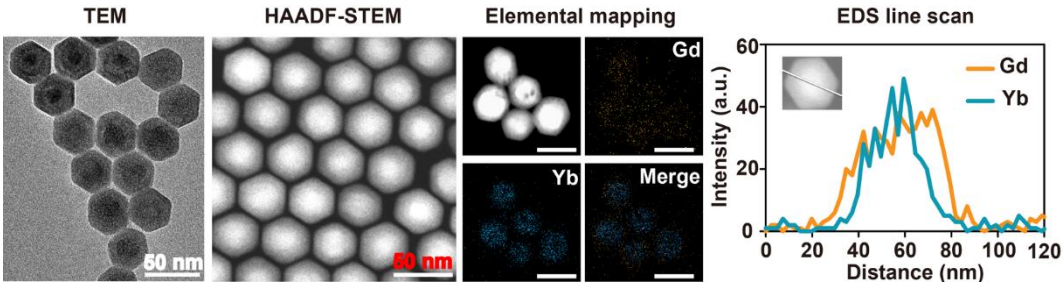

Figure S5. TEM image, HAADF-STEM image, elemental mapping image, and EDS line scan profile of $NaGdF_4$:70%Yb,1%Tm@$NaGdF_4$ core-shell UCNPs.

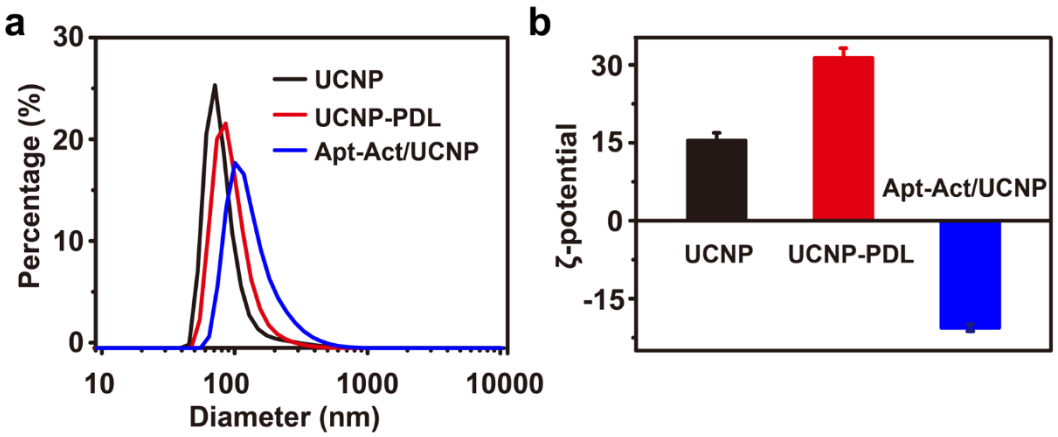

Figure S6 Monitoring the (a) hydrodynamic size distribution and (b) zeta potential during the synthesis of Apt-Act/UCNPs. The integration of Apt-Act probes on the UCNPs was further confirmed by dynamic-light-scattering (DLS) analysis and zeta potential measurement at each step during the synthesis. DLS analysis revealed that the average size of the OA-free UCNPs was increased from ~84 nm to ~92 nm and ~129 nm after the PDL coating and subsequent DNA loading, respectively. Zeta potential measurement at each step showed that the positively charged UCNPs (+15.4 mV) became more positively charged with the coating of PDL (+31.3 mV) and then negatively charged after loading with Apt-Act probes (-20.6 mV).

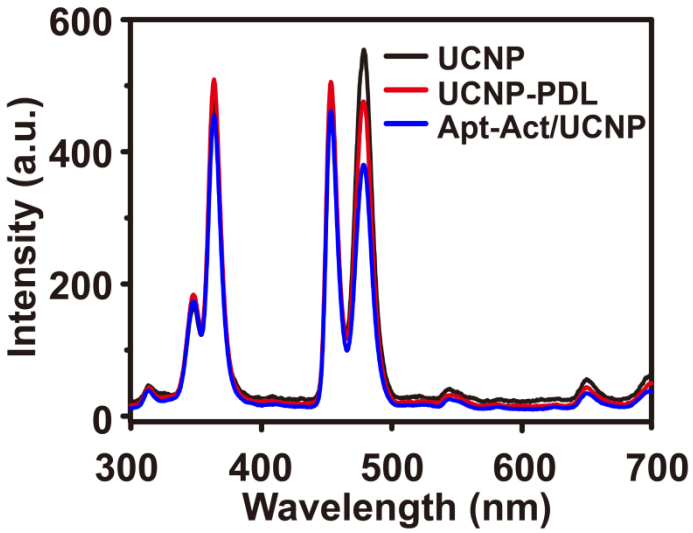

Figure S7. Upconversion luminescence spectra of the UCNP-based samples under excitation at 980 nm. The Apt-Act/UCNPs display characteristic Tm^{3+} dominated UV (320 and 360 nm) and visible blue (450 and 475 nm) UCL under excitation at 980 nm, corresponding to the $^3P_6 \rightarrow {}^3F_4$, $^1D_2 \rightarrow {}^3H_6$, $^1D_2 \rightarrow {}^3F_4$, and $^1G_4 \rightarrow {}^3F_4$ transitions, respectively.[5]

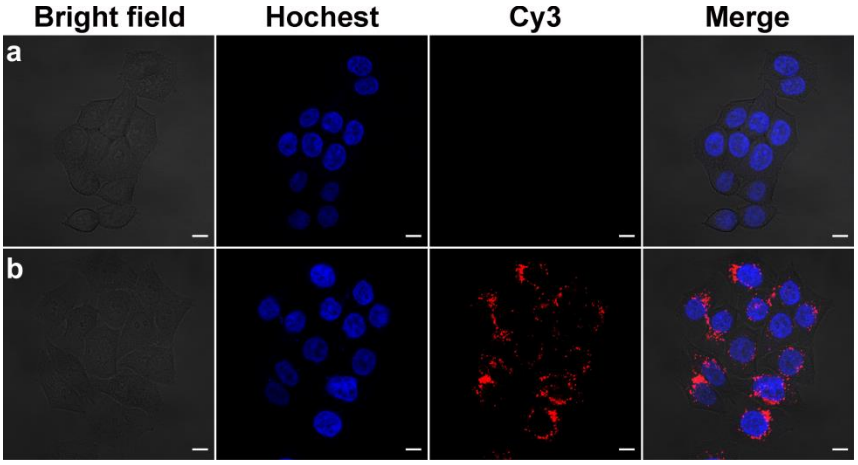

Figure S8. Confocal fluorescence images of HeLa cells treated with (a) Apt-Act and (b) Apt-Act/UCNPs.

Scale bar: 10 μm.

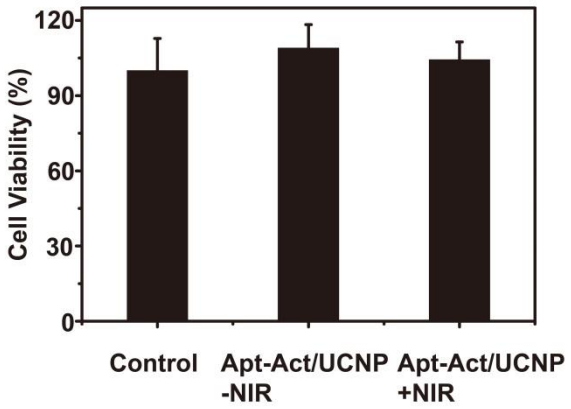

Figure S9. Cell viability of HeLa cells treated with Apt-Act/UCNPs, and with/without NIR irradiation.

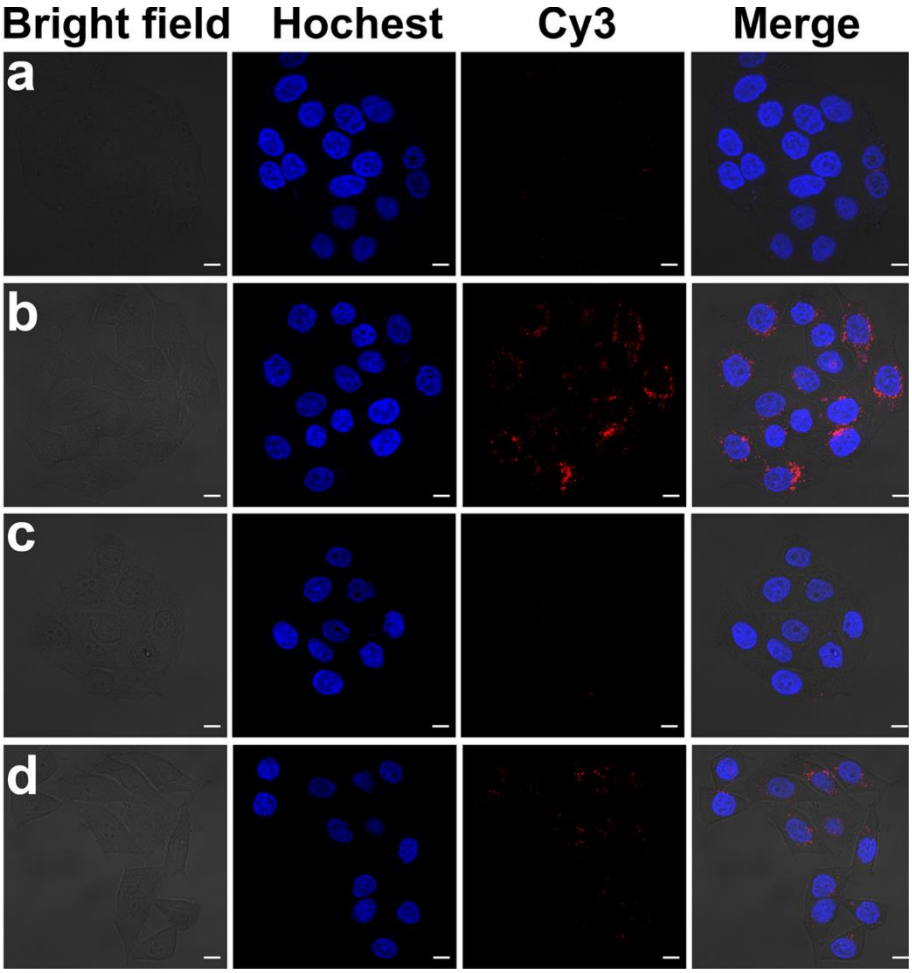

Figure S10. Confocal fluorescence images of HeLa cells treated with (a) Apt-Act/UCNPs, (b) Apt-Act/UCNPs + NIR, (c) IAA + Apt-Act/UCNPs, (d) IAA + Apt-Act/UCNPs + NIR. Scale bar: 10 μm.

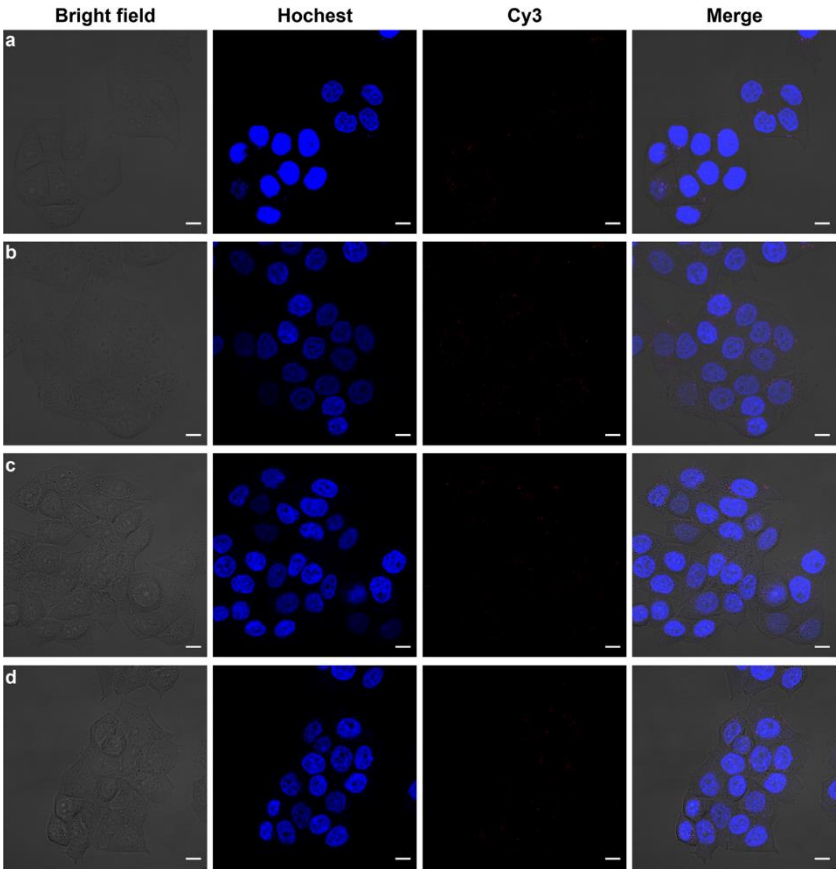

Figure S11. Confocal fluorescence images of HeLa cells treated with (a) Apt-non/UCNPs, (b) Apt-non/UCNPs + NIR, (c) IAA + Apt-non/UCNPs, (d) IAA + Apt-non/UCNPs + NIR. Scale bar: 10 μm.

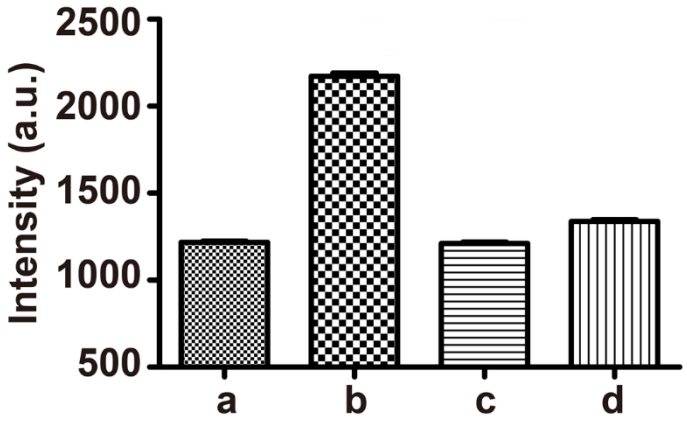

Figure S12. Flow cytometric quantification of fluorescence of HeLa cells treated with (a) Apt-Act/UCNPs, (b) Apt-Act/UCNPs + NIR, (c) Apt-non/UCNPs, (d) Apt-non/UCNP + NIR. Data are medians ± quartiles, n = 4.

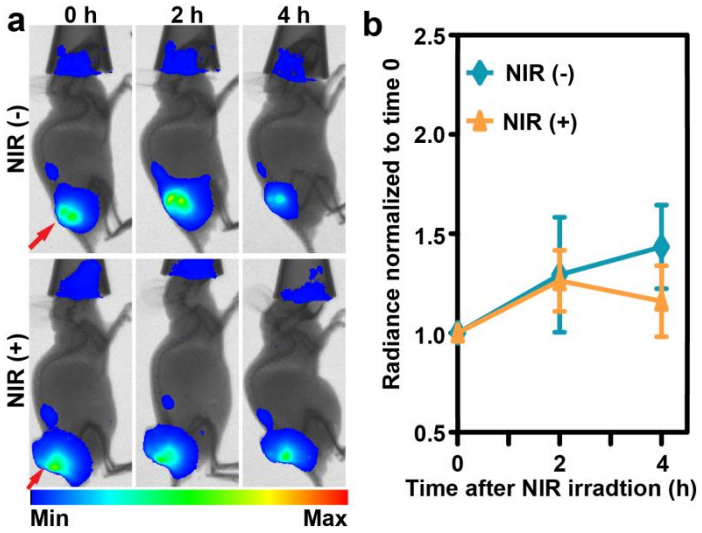

Figure S13. (a) Representative fluorescence images of HeLa tumor-bearing mice injected with Apt-non/UCNPs without or with subsequent NIR irradiation at the tumor site. Arrows indicate the sites of tumors. (b) Effects of NIR irradiation on ATP sensor activity of the Apt-non/UCNPs in tumor over time; data normalized to fluorescence signal at 0 h. Data are medians ± quartiles, n = 4.

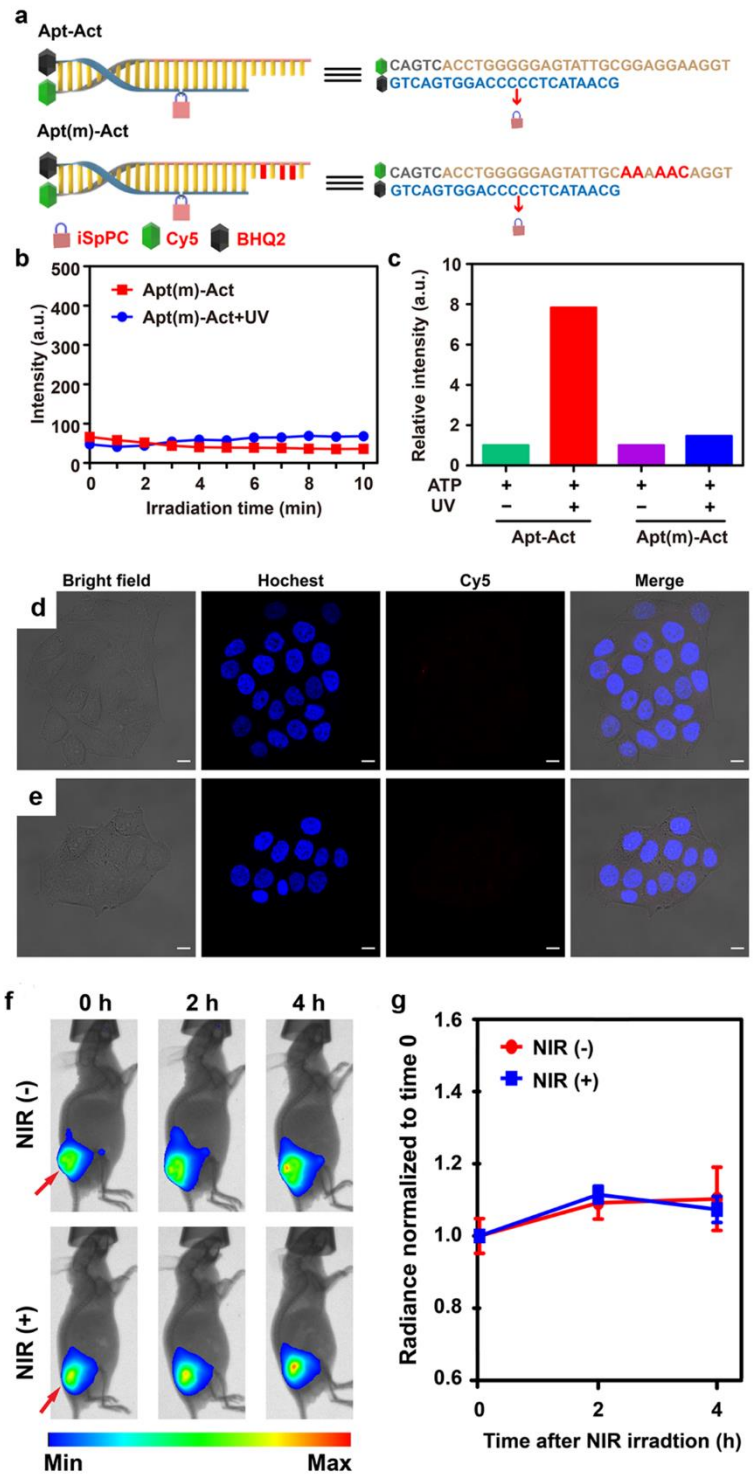

Figure S14. (a) The molecular structure of Apt-Act and Apt(m)-Act probe, respectively. (b) Fluorescence spectra of the Apt(m)-Act probe by increasing doses (in minutes) of 365 nm light, in response to 5 mM ATP. (c) Response of the Apt-Act probe and Apt(m)-Act probe to ATP (5 mM) and UV light (365 nm), respectively.

Confocal fluorescence images of HeLa cells treated with (d) Apt(m)-Act/UCNPs and (e) Apt(m)-Act/UCNPs + NIR. (f) Representative fluorescence images of HeLa tumor-bearing mice injected with Apt(m)-Act/UCNPs without or with subsequent NIR irradiation at the tumor site. Arrows indicate the sites of tumors. (g) Effects of NIR irradiation on ATP sensor activity of the Apt(m)-Act/UCNPs in tumor over time; data normalized to fluorescence signal at 0 h. Data are medians ± quartiles, n = 4.

As a control, some crucial nucleotides in the aptamer strand in the Apt-Act probe are mutated to yield Apt(m)-Act probe (Figure S14a). No obvious change in fluorescence intensity was observed for Apt(m)-Act in the presence of 5 mM ATP and UV light irradiation (Figure S14b,c), indicating that the ATP sensing activity was inhibited through the aptamer sequence mutation. Furthermore, NIR-activated ATP sensing was not observed for the Apt(m)-Act/UCNPs in living cells and in vivo (Figure S14d-g). The experiment eliminated the potential artifacts, particularly in cells/in vivo, that result from unexpected removal of the PC-inhibitor strand.

Reference

[1] Mai, H. X.; Zhang, Y. W.; Si, R.; Yan, Z. G.; Sun, L. D.; You, L. P.; Yan, C. H. *J. Am. Chem. Soc.* **2006**, *128*, 6426.

[2] Boyer, J.-C.; Vetrone, F.; Cuccia, L. A.; Capobianco, J. A. *J. Am. Chem. Soc.* **2006**, *128*, 7444.

[3] Zhang, F.; Che, R.; Li, X.; Yao, C.; Yang, J.; Shen, D.; Hu, P.; Li, W.; Zhao, D. *Nano Lett.* **2012**, *12*, 2852.

[4] Verrax, J.; Dejeans, N.; Sid, B.; Glorieux, C.; Calderon, P. B. *Biochem. Pharmacol.* **2011**, *82*, 1540.

[5] Dong, H.; Du, S.-R.; Zheng, X.-Y.; Lyu, G.-M.; Sun, L.-D.; et al. *Chem. Rev.* **2015**, *115*, 10725.